ELSEVIER

Journal of Nuclear Materials 254 (1998) 1–8

journal of nuclear materials

Clustering and ordering of nitrogen in nuclear grade 316LN austenitic stainless steel

P. Shankar [*], D. Sundararaman [1], S. Ranganathan [2]

Metallurgy Division, Indira Gandhi Centre for Atomic Research, Kalpakkam 603102, India

Received 30 May 1997; accepted 28 November 1997

Abstract

The high misfit strains associated with nitrogen addition and the high chemical affinity with chromium result in a significant driving force for the formation of Cr–N clusters in austenitic steels. The microstructural signatures of cluster formation in nuclear grade 316LN austenitic stainless steel during the early stages of aging at 1123 K are discussed. Aging beyond 25 h results in transformation of fcc clusters to hexagonal Cr_2N precipitates. Strain induced ordering of nitrogen in Cr_2N precipitates due to continued ageing is also highlighted. © 1998 Elsevier Science B.V.

1. Introduction

Nitrogen steels are becoming an important class of engineering materials by virtue of their superior chemical and mechanical properties. 316LN austenitic stainless steels with about 0.08 wt% nitrogen are recognized as the candidate structural material for fast breeder reactors. Nitrogen is found to have a strong influence on the tensile, fatigue, creep and corrosion behavior of austenitic steels. The sensitive dependence of the engineering properties on the interstitial content even when present only in dilute concentrations stems from its ability to influence the fine-scale microstructural state of the material.

The thermodynamic stability and microstructural evolution in interstitial systems are largely governed by the stress induced interactions, rather than chemical energy factors. The stress is generated as a consequence of the volume misfit between the octahedral void size in austenite and the size of interstitial atoms occupying them. The influence of stress induced interactions on clustering and ordering of nitrogen in the Ti–N system have been well documented [1]. Atomistic theories developed by Khachaturyan [2] and Cook [3] clearly bring out the tendency for strain induced ordering even at surprisingly low concentrations of interstitial solute of the order of 0.1 to 0.5 at.%. The chemical and mechanical properties will therefore be largely influenced by the exact nature of strain field contours in the system.

Further, although carbon and nitrogen are both interstitials, they have different magnitudes of influence on the properties, particularly in austenitic stainless steel. The misfit strain associated with nitrogen alloying is found to be larger than that induced by alloying with carbon. The coefficient of lattice dilation of austenite matrix by nitrogen is higher than that caused by carbon [4]. This is in spite of the fact that the atomic radius of a nitrogen atom is smaller than that of a carbon atom, thereby the misfit strain would have otherwise been expected to be lower for nitrogen steels than carbon steels. Also, it is found that nitrogen has a higher tendency for pinning dislocations in austenitic stainless steels than carbon [5]. Hence, in general, it is found that nitrogen extends a greater influence on the mechanical properties of austenitic steels. It is obvious, therefore, that the electronic structure and chemical bonding also play an important role, apart from the strain induced interactions, in deciding the degree of microchemical repartitioning and precipitation of metastable phases.

[*] Corresponding author.

[1] Present address: Institute of Space and Astronautical Science, 3-1-1, Yoshinodai, Sagamihara, Kanagawa 229, Japan.

[2] Present address: Centre for Advanced Study, Department of Metallurgy, Indian Institute of Science, Bangalore 560 012, India.

PII S0022-3115(97)00357-7

Many hypotheses have been proposed to account for the influence of nitrogen on the mechanical properties of austenitic steels. These include (a) formation of Cr–N clusters, (b) formation of short-range ordered zones and (c) decrease of stacking fault energy by addition of nitrogen. The formation of Cr_2N precipitates on thermal aging have been reported both in nuclear grade 316LN steels by the present authors [6] and also in high nitrogen steels by others [7,8]. However, there has not been any detailed electron microscopic characterization of pre-precipitation effects even in high nitrogen steels. The only evidences of complexes at room temperature in alloys containing more than 0.16 wt% nitrogen have been reported based on extended X-ray absorption fine structure (EXAFS) analysis [9] and field ion microscopy (FIM) investigations [10]. The ordering of nitrogen in chromium nitride precipitates is also a less widely studied phenomenon. The emphasis of the present paper will be to characterize the microstructural signatures associated with early stages of Cr–N clustering and the subsequent precipitation of interstitially ordered nitrides in nuclear grade 316LN austenitic stainless steels.

2. Experimental procedure

The composition of the nuclear grade 316LN austenitic stainless steel characterized in the present study is given in Table 1. The as-received steel plates were rolled into thin sheets of about 100 μm and were subsequently solution annealed (SA) at 1523 K for 0.5 h, in a high temperature vacuum furnace. SA samples were encapsulated in quartz tubes evacuated to about 10^{-8} bar and aged in a muffle furnace at 1123 K for various time durations ranging from 2 h to 2000 h. Specimens for transmission electron microscopy (TEM) were thinned electrolytically in a solution of 5% perchloric acid in methanol. The cell potential was maintained at 22 V and the bath temperature was kept below 273 K. Samples were observed in a Philips 400T and JEOL 2000 EX II TEM.

X-ray diffraction (XRD) characterization of the SA and aged specimens were performed to qualitatively monitor the variations in the interplanar spacing of austenite. A Philips diffractometer with Cu Kα radiation fitted with a curved graphite crystal monochromator in the diffracted beam direction was employed for this purpose.

Table 1
Composition in weight percent of the nuclear grade 316LN stainless steel characterized

C	N	S	Ni	Cr	Mo	Mn	Fe
0.021	0.078	0.002	11.9	16.9	2.3	1.3	rest

3. Results and discussion

TEM investigations of Cr_2N precipitation on thermal aging of these steels at 1123K beyond 25 h have been reported by the present authors elsewhere [11]. The only microstructural features associated with intra-granular Cr_2N precipitation were found to be the presence of dislocation pairs in aged specimens in contrast to the random dislocation structure in SA specimens. On continued aging a change from intra-granular precipitation to cellular precipitation mode has been reported [12].

Cr_2N has a hexagonal crystal structure and can exist in two forms. Type-A Cr_2N is an interstitially disordered phase having lattice parameter of $a_A = 0.2748$ nm and $c_A = 0.4438$ nm [13]. In type-B Cr_2N, nitrogen is ordered in the interstitial sub-lattice. Lattice parameter of the ordered chromium nitride is $a_B = 0.476$ nm and $c_B = 0.4438$ nm [14]. The electron diffraction patterns associated with Cr_2N precipitation [11,12] reported earlier could be indexed to both the types of Cr_2N. Further the superlattice spots because of nitrogen ordering coincided with the double diffraction spots, leaving the ambiguity of conclusively determining the state of order of the system by electron diffraction analysis alone. In the following sections, the new results of further studies on pre-precipitation behavior and nitrogen ordering in Cr_2N are presented.

3.1. Cr–N clusters in austenite

TEM observations showed a mottled contrast during the early stages of aging up to 25 h, as shown in Fig. 1. This indicates the possible formation of interstitial–substitutional complexes in the matrix. The high lattice strains induced by nitrogen, complimented with its very high negative enthalpy of binding with Cr can result in a high driving force for the formation of Cr–N clusters in austenite matrix. The nitrogen atoms occupy the octahedral void site in fcc and are surrounded by six nearest neighbor

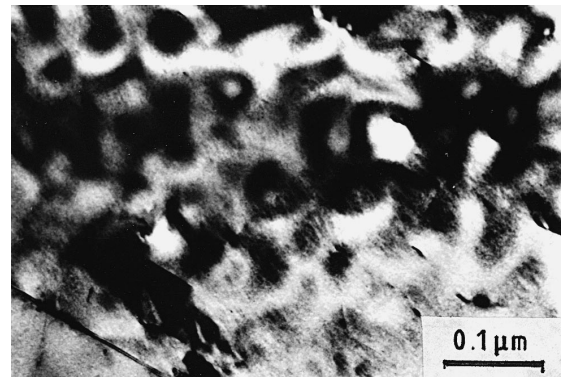

Fig. 1. Mottled contrast in specimen aged for 10 h at 1123 K, indicative of solute clustering.

metal atoms in substitutional lattice sites. Thermodynamic calculations by Grujicic and Owen [15], have indicated more than 80% probability of nitrogen atoms being surrounded by three or more Cr atoms as its first neighbors. The formation of such clusters is composed of kinetically constrained processes as they involve diffusion of Cr and N species.

These clusters would still have only the same fcc structure of austenite, although there would be differences in their lattice parameter, owing to the local composition fluctuations. Dark field images from regions showing mottled contrast, showed the presence of fine fringes distributed in the matrix as shown in Fig. 2(a, b). Similar platelet type defect features have also been observed in nitrogen doped diamonds [16,17]. TEM characterizations of these defect features lying on {100} planes have been reported and have been seen to be in the size ranges of about 20 to 100 nm. It is to be realized that nitrogen in diamond is a substitutional solute. However, localized segregation of nitrogen can result in lattice strains. Localized fluctuations in lattice parameter arising from chemical heterogeneities can result in these features appearing as moire type fringes in the matrix. In the 316LN stainless steel specimen observed in the present study, the density of such platelet type defects showed a maximum at about 10 h of aging time. Strain contours associated with such fine scale repartitioning of nitrogen atoms can also be seen in Fig. 2(b). Strain induced interaction between platelet defects is also commonly observed, resulting in formation of arrays or network structures as can be seen from the micrograph.

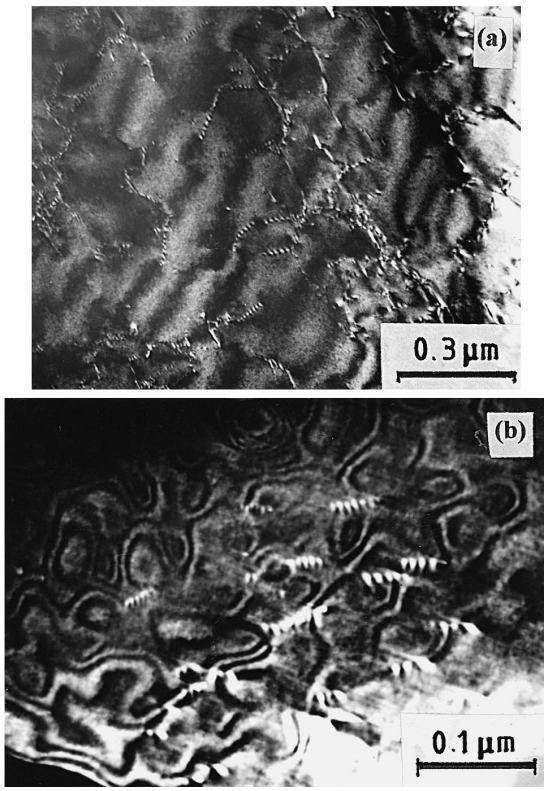

Fig. 2. (a) Cr–N clusters in austenite matrix observed as fine fringes in the dark field image. (b) Strain contours associated with fine scale repartitioning of interstitial elements during cluster formation.

Localized variations in chemical composition could have two types of effects on the high resolution lattice image. It will influence the contrast and also the fringe spacing. The scattering factor from a given volume of material is a sensitive function of the chemical species of which it is composed of. Changes in composition will therefore significantly alter the phase contrast. Hence, by choosing an appropriate reflection that is most sensitive to chemical composition fluctuations (chemical reflections), the impact of chemical lattice imaging on quantitative composition mapping of materials with near atomic resolution and sensitivity has been demonstrated [18]. This technique is particularly advantageous in ordered phases. Chemically disordered phases do not possess any chemical reflections and hence this technique may not be very handy. The second method of chemical composition estimation from high resolution lattice imaging by fringe spacing measurements can however be employed to chemically disordered phases as well. This technique is based on Vegard's law, assuming the lattice parameter to be a linear function of the solute concentration. Fringe spacing modulations in high resolution lattice images have been used to study the spinodal decomposition in the Au–Ni [19] system and also to study the concentration gradient at a grain boundary precipitate/matrix interface in the Al–Zn system [20]. In an Fe–2%Si–0.1%C alloy having alpha/martensitic structure, the carbon segregation in martensite has been estimated to be 0.6% by this technique [21]. In contrast to other techniques like EELS, EDAX, microdiffraction and CBED, HREM lattice imaging exclusively depends only on the imaging mode and thereby has the unique advantage of high spatial resolution (2A°). Highly localized composition fluctuations even at atomic plane level can be estimated by this technique. HREM is therefore a versatile tool, particularly for studying the early stages of precipitation. The sensitivity of fringe spacing modulation technique would be particularly very useful in studying the pre-precipitation reactions in interstitial systems. The strong dependence of lattice parameter on interstitial concentration dependence, results in greater accuracy and dependency of this technique in estimating trends in concentration fluctuations in matrix.

High resolution lattice images indicative of the presence of clusters in a specimen aged for 10 h are shown in Fig. 3(a, b). Regions with localized differences in their lattice parameter can be clearly seen from the high resolution images. This can occur only as a consequence of highly localized fluctuations in solute concentrations. These

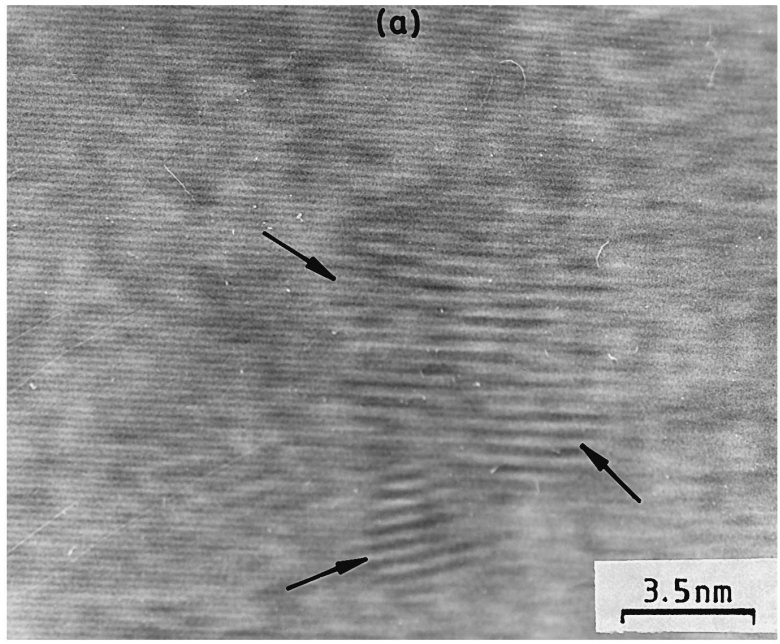

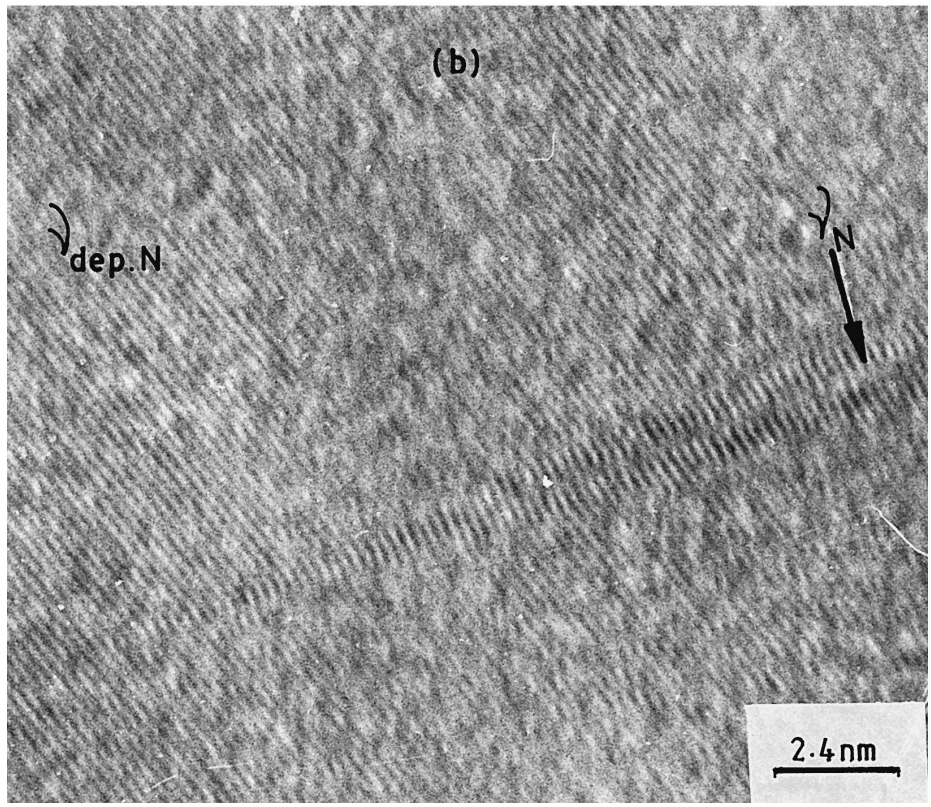

Fig. 3. (a) HREM lattice image of {111} planes showing a network of Cr–N clusters in austenite matrix. (b) HREM lattice image of {111} planes showing highly localized segregation of nitrogen, in austenite matrix. 'γ_N' corresponds to region enriched with nitrogen; while '$\gamma_{dep.N}$' corresponds to the matrix region depleted with nitrogen. The 0.01111 nm difference between nitrogen segregated regions and the matrix correspond to about 22.4 at.% nitrogen concentration in these regions.

regions of local disturbances are seen to be only a few atomic layers thick. By mass density calculations employing XRD and the Archimedes principle in a wide number of alloys with different carbon and nitrogen levels and by using the least square fitting procedure, the following dependence of lattice parameter (a) has been proposed [4]:

$$a\,(\mathrm{nm}) = a_0 + 0.000783\,X_C + 0.000861\,X_N,$$

where X_C and X_N denote fractional compositions of carbon and nitrogen, respectively. The lattice parameter of austenite increases at a rate of 0.000861 nm per atom percent of nitrogen added. The differences between the {111} interplanar spacing of the depleted matrix and the segregated region shown in Fig. 3(b) is found to be approximately 0.01111 nm. This corresponds to a lattice parameter variation of 0.019244 nm. If it is assumed that this is primarily due to nitrogen segregation alone, then this could suggest a concentration of about 22.4 at.% nitrogen in the clusters. However, it is to be realized that this technique based on fringe spacing modulation correlation, cannot distinguish between composition fluctuations and locked-in elastic strains. Since the present study deals only with solution annealed and thermally aged specimens, all other contributions to strain can be neglected. Also, it is known that variations in substitutional solute concentration do not significantly alter the lattice parameter. Therefore, the assumption of the lattice parameter change to be attributed primarily only to nitrogen repartitioning is not unreasonable. Localized segregations of nitrogen to such a large extent would undoubtedly have a remarkable influence on the austenite matrix lattice parameter.

XRD investigations of SA and aged specimens were carried out to qualitatively observe the trend in change of austenite lattice parameter by monitoring the {113} peak of austenite. The results of the XRD studies are presented in Fig. 4. A drastic decrease in the interplanar spacing of austenite is observed during the early stages of ageing. This is in good agreement with the TEM observation of cluster formation, associated with matrix depletion of chromium and nitrogen solutes.

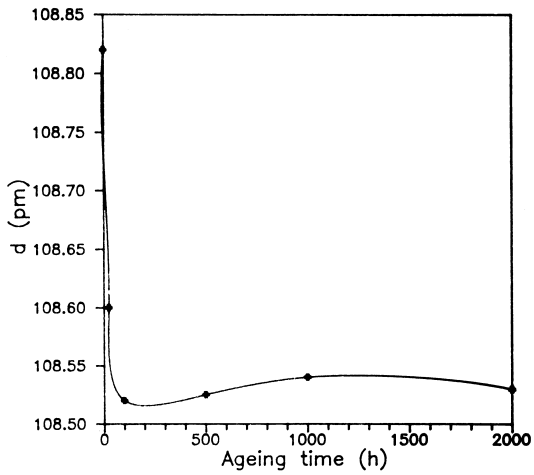

Fig. 4. Influence of thermal aging on interplanar spacing of parameter of austenite estimated by XRD.

However, it is to be mentioned that the state of chemical order of nitrogen in the fcc clusters cannot be inferred from the electron microscopy methods. The very low scattering amplitudes of nitrogen would mask the contrast variations arising out of ordering reactions. Also the nitrogen atoms cannot be directly imaged by HREM [1] and thereby adds to the difficulty in ascertaining whether the Cr–N rich clusters are chemically ordered or not.

3.2. Interstitially ordered Cr_2N precipitate

Aging beyond 25 h, results in the precipitation of intra-granular Cr_2N. Based on the misfit strain analysis [11], it was concluded that type-A Cr_2N is the first to nucleate, which then subsequently undergoes nitrogen ordering. Careful electron diffraction experiments did result in reciprocal lattice sections which could be indexed based on type-B interstitially ordered Cr_2N only. The SAD patterns from region containing dislocation pairs showing their association with precipitation of ordered Cr_2N, along with its key, are shown in Fig. 5(a, b). The {1010} type reflections indicated in Fig. 5(b) do not have any equivalent reflections from the disordered nitride phase. This can be contrasted with the reciprocal lattice sections reported earlier [11,12], which could be indexed to both the ordered as well as the disordered Cr_2N structure, as shown in Fig. 5(c, d). The (1010) reflections from type-A Cr_2N could also be indexed equally well as (1120) reflections from type-B Cr_2N. The reciprocal lattice section shown in Fig. 5(a) can, however, be unequivocally indexed to ordered Cr_2N only. The tendency for pairing of dislocations can then be easily understood, as a consequence of minimizing the energy. Strain induced interactions also result in the dislocation pair to form network structures as shown in Fig. 5(e).

A transition from interstitially disordered to ordered intragranular precipitation of chromium nitrides has been reported earlier by the present authors [11]. Based on misfit strain analysis, this transition has been predicted to occur during the period between 25 to 100 h of aging. The high strain energy introduced as a result of interstitial nitrogen drives the ordering phenomenon to result in a lower energy state. The disordered Cr_2N will obviously have a higher free energy than the ordered state and therefore would also have higher solubility of solutes in the matrix, as shown schematically in Fig. 6. Interstitial ordering would therefore be accompanied by a further depletion of matrix solute elements, although to a lesser extent when compared to that caused by clustering in the matrix. Fig. 7 gives an enlarged representation of Fig. 4 for aging times up to 100 h. In accordance with the

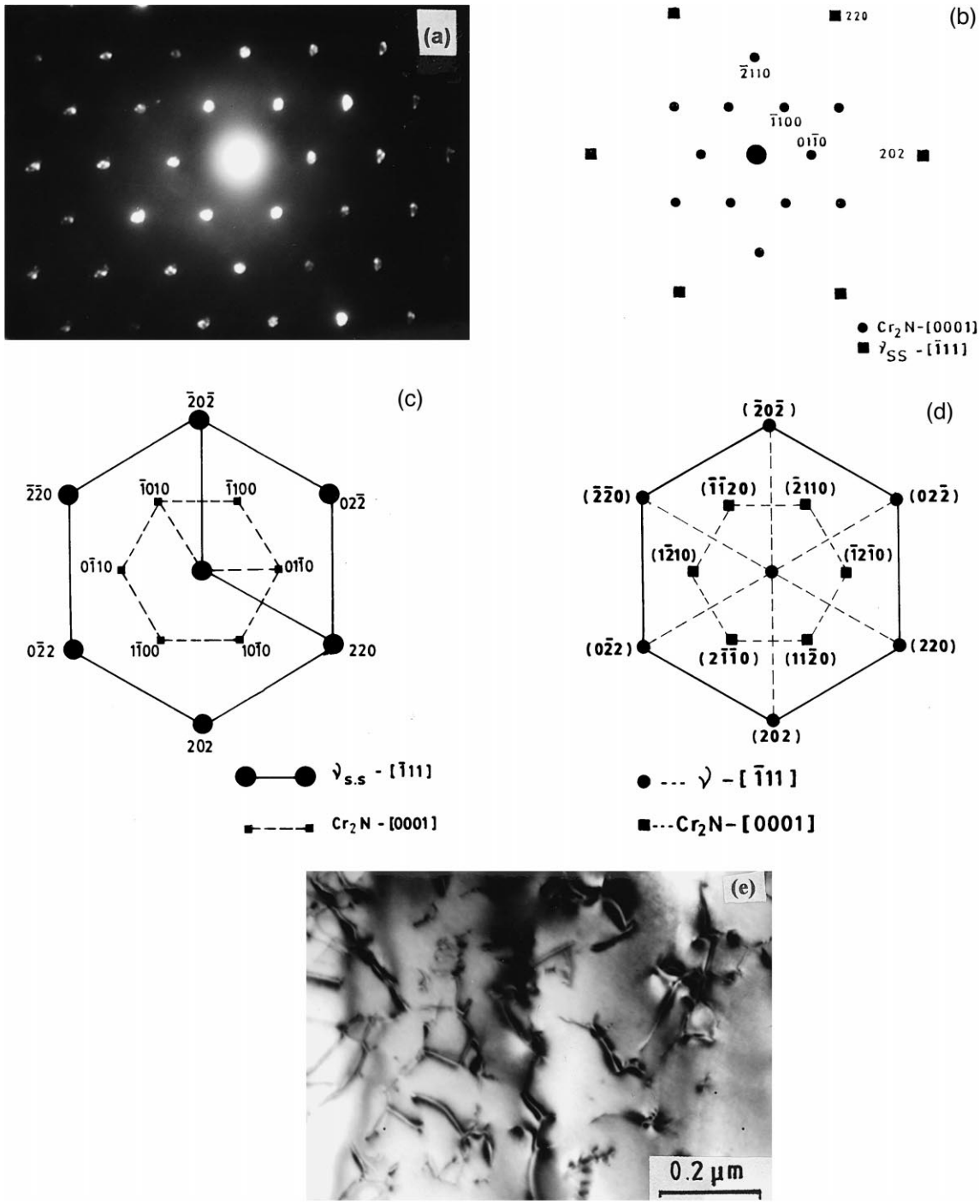

Fig. 5. SAD pattern from regions containing dislocation pairs and its key are shown in (a, b), unambiguously concluding the presence of ordered Cr_2N. The SAD pattern presented previously [11,12], could be indexed to both type-A, as well as type-B ordered Cr_2N, as shown in (c, d), respectively. The (1010) reflection from type-A can also be indexed as equivalent to (1120) reflection from type-B Cr_2N. (e) Bright field image showing interaction of dislocation pairs leading to formation of network structures.

expectations, it can be seen that the interplanar spacing of austenite continues to decrease even beyond 25 h of aging up to 100 h. This suggests a further depletion of nitrogen from the austenite matrix primarily during the time period associated with disordered to ordered phase transformation. However, the rate of solute depletion from matrix

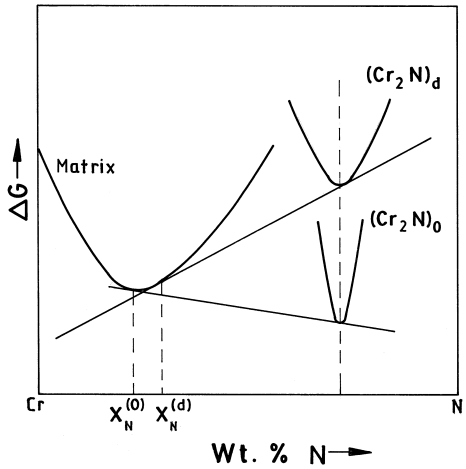

Fig. 6. Schematic of the Gibbs energy-composition diagram showing the higher solubility of the solute (N) in the matrix in equilibrium with disordered Cr_2N (X_N^d) as compared to its solubility when in equilibrium with the ordered precipitate (X_N^o).

during the ordering reaction can be seen to be much less than that occurring during the stages of Cr–N cluster formation in the matrix. On continuing aging beyond 100 h, the volume fraction of the chromium nitrides is almost constant, although there is a change from intragranular to cellular precipitation mode. The austenite lattice parameter therefore saturates beyond 100 h of aging.

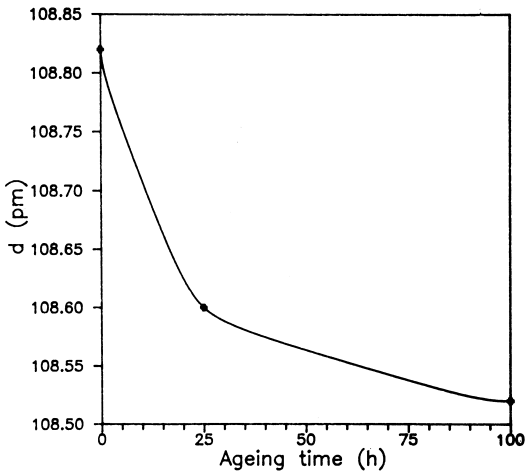

Fig. 7. Magnified representation of Fig. 4, showing two slope behavior of interplanar spacing variation of austenite on aging up to 100 h. Note the continued decrease in interplanar spacing on aging between 25 and 100 h, associated with the ordering of intra-granular Cr_2N precipitates.

4. Conclusions

(i) The presence of platelet defects in matrix on ageing up to 25 h at 1123 K is associated with the formation of Cr–N clusters.

(ii) Based on fringe spacing modulation from HREM lattice images, the extent of nitrogen segregation in clusters is estimated to be about 22 at.%.

(iii) Conclusive electron diffraction evidences of nitrogen ordering in Cr_2N have been presented.

(iv) Strain induced interactions often lead to formation of network structures of both clusters and ordered precipitates.

Acknowledgements

The authors are grateful to Dr Placid Rodriguez (Director, IGCAR) and Dr Baldev Raj (Director, Metallurgy and Materials Group, IGCAR) for their inspiration and encouragement given to carry out this work. The authors also thank Dr V.S. Raghunathan (Head, Metallurgy Division, IGCAR) for useful comments on the manuscript.

References

[1] D. Sundararaman, S. Ranganathan, V.S. Raghunathan, Metall. Mater. Trans. 27A (1966) 2966.
[2] A.G. Khachaturyan, Sov. Phys. Solid State 9 (1968) 2249.
[3] H.E. Cook, D. deFontaine, Acta Metall. 17 (1969) 915.
[4] H.M. Ledbetter, M.W. Austin, Mater. Sci. Tech. 3 (1987) 101.
[5] V.G. Gavriljuk, V.A. Duz, S.P. Jephimenko, Proc. Int. Conf. On High Nitrogen Steels, HNS'88, Lille, France, 1988, J. Foct, A. Hendry (Eds.), The Institute of Metals, London, 1989, p. 447.
[6] P. Shankar, D. Sundararaman, V.S. Raghunathan, S. Ranganathan, Trans. Ind. Inst. Metal. 48 (1995) 237.
[7] E. Ruedl, G. Valdre, J. Mater. Sci. 23 (1988) 3698.
[8] M. Kikuchi, M. Kajihara, S. Choi, Mater. Sci. Eng. A 146 (1991) 131.
[9] K. Oda, N. Kondo, K. Shibata, J. Iron Steel Inst. Jpn. 30 (1990) 625.
[10] G. Wahlberg, U. Rolander, H.O. Andren, Proc. Int. Conf. On High Nitrogen Steels, HNS'88, Lille, France, 1988, J. Foct, A. Hendry (Eds.), The Institute of Metals, London, 1989, p. 163.
[11] D. Sundararaman, P. Shankar, V.S. Raghunathan, Metall. Trans. 27A (1996) 1175.
[12] P. Shankar, D. Sundararaman, S. Ranganathan, Scr. Metall. Mater. Trans. 31 (1994) 589.
[13] K.W. Andrews, D.J. Dyson, S.R. Keown, Interpretation of Electron Diffraction Patterns, Hilger, London, 1971, p. 203.
[14] P. Villas, L.D. Calvert, Pearson's Handbook of Crystallographic Data for Intermetallic Phases, ASM, Metals Park, OH, 1985, p. 1877.
[15] M. Grujicic, W.S. Owen, Acta Metall. Mater. 43 (1995) 4201.

[16] N. Sumida, A.R. Lang, Proc. R. Soc. London A 419 (1988) 235.
[17] N. Sumida, A.R. Lang, J. Appl. Cryst. 15 (1982) 266.
[18] A. Ourmazd, F.H. Baumann, M. Bode, Y. Kim, Ultramicroscopy 34 (1990) 237.
[19] R. Sinclair, R. Gronsky, G. Thomas, Acta Metall. 24 (1976) 789.
[20] R. Gronsky, G. Thomas, Proc. 35th Annual Meeting of Electron Microscopy Society of America, Claitors, Baton Rouge, LA, 1977, p. 116.
[21] J.Y. Koo, G. Thomas, Proc. 35th Annual Meeting of Electron Microscopy Society of America, Claitors, Baton Rouge, LA, 1977, p. 118.